Development 133, 3767-3775 (2006) doi:10.1242/dev.02552

BMP signaling in the epiblast is required for proper recruitment of the prospective paraxial mesoderm and development of the somites

Shigeto Miura[1], Shannon Davis[2], John Klingensmith[2] and Yuji Mishina[1,*]

Bmpr1a encodes the BMP type IA receptor for bone morphogenetic proteins (BMPs), including 2 and 4. Here, we use mosaic inactivation of *Bmpr1a* in the epiblast of the mouse embryo (*Bmpr-MORE* embryos) to assess functions of this gene in mesoderm development. Unlike *Bmpr1a*-null embryos, which fail to gastrulate, *Bmpr-MORE* embryos initiate gastrulation, but the recruitment of prospective paraxial mesoderm cells to the primitive streak is delayed. This delay causes a more proximal distribution of cells with paraxial mesoderm character within the primitive streak, resulting in a lateral expansion of somitic mesoderm to form multiple columns. Inhibition of FGF signaling restores the normal timing of recruitment of prospective paraxial mesoderm and partially rescues the development of somites. This suggests that BMP and FGF signaling function antagonistically during paraxial mesoderm development.

KEY WORDS: Epiblast, Primitive streak, Paraxial mesoderm, Somites, BMP, FGF, Mouse

INTRODUCTION

Gastrulation begins around embryonic day 6.5 (E6.5), when the primitive streak, a transient structure, forms in the posterior epiblast at its junction with the extra-embryonic ectoderm. As gastrulation progresses, cells are recruited to intercalate between the proximal and the distal ends of the primitive streak, and ultimately the primitive streak extends to the distal tip of the egg cylinder (Tam and Behringer, 1997). In this case, 'proximal' refers to the end of the primitive streak closest to the extra-embryonic tissues. At the early to mid streak stage, primarily future extra-embryonic mesodermal cells are recruited to the proximal primitive streak and they are committed to yolk sac mesoderm (Kinder et al., 1999; Lawson et al., 1991; Parameswaran and Tam, 1995). By the late streak stage, prospective lateral plate mesoderm (LPM) and paraxial mesoderm (PXM) cells are recruited to the middle and anterior primitive streak, respectively, and become committed to trunk mesoderm (Kinder et al., 1999; Parameswaran and Tam, 1995; Tam and Quinlan, 1996). However, the molecular mechanisms involved in recruitment of the epiblast cells are largely unknown (Tam and Behringer, 1997).

It is now well established that BMP signaling regulates the development of many embryonic cell types, including the heart and hematopoietic tissues (Kishigami and Mishina, 2005; Mishina, 2003). The development of the lateral plate is also regulated by BMP signaling. Hensen's node or the BMP antagonist Noggin can generate somites from lateral plate cells (Hornbruch et al., 1979; Tonegawa and Takahashi, 1998). Thus, BMP signaling plays a role in patterning the LPM. In addition to BMPs, other growth factors are crucial for somitic development. For example, fibroblast growth factor receptor 1 (*Fgfr1*) deficient embryos do not form somites, and FGF signaling is involved in the development of the PXM lineage (Ciruna and Rossant, 2001; Yamaguchi et al., 1994). Thus, one can speculate that there is a high potential for interaction between BMP and FGF signaling during mouse mesoderm development. However, little is known about how they might interact to regulate paraxial versus other mesodermal tissues.

Bmpr1a encodes the type 1 BMP receptor BMPR1A, which is known to be a receptor for BMP2 and BMP4 (Mishina, 2003). These molecules constitute a major BMP signaling component in early mouse development. However, because *Bmpr1a*-null mutant embryos do not initiate gastrulation (Mishina et al., 1995), the function of *Bmpr1a* during gastrulation in mice is largely unknown. To elucidate functions of BMP signaling through BMPR1A during and after gastrulation, we have generated a conditional allele of *Bmpr1a* (Mishina et al., 2002). The *Mox2-Cre* (MORE) strain drives mosaic *Cre*-mediated recombination in the epiblast, providing a useful tool for reducing but not completely abolishing gene expression in the epiblast (Hayashi et al., 2002; Tallquist and Soriano, 2000). For simplicity, we refer to embryos in which *Bmpr1a* is ablated as a result of MORE activity as *Bmpr-MORE* embryos. Our previous studies using *Bmpr-MORE* embryos showed that the anterior neural ectoderm was enlarged at the expense of surface ectoderm, and that endodermal morphogenesis was defective (Davis et al., 2004). Here, the development of mesodermal tissues is studied in *Bmpr-MORE* embryos. The results indicate that *Bmpr1a* in the epiblast is required to regulate the recruitment of prospective PXM cells correctly and consequently to direct normal somite development. Our results also indicate that BMP and FGF signaling interact for proper development of the mesoderm during gastrulation.

MATERIALS AND METHODS

Mouse

The strain information and genotyping procedures were described previously (Davis et al., 2004). All mouse experiments were performed in accordance with NIH and institutional guidelines covering the humane care and use of animals in research.

[1]Laboratory of Reproductive and Developmental Toxicology, National Institute of Environmental Health Sciences, 111 T. W. Alexander Drive, PO Box 12233, MD C4-10, C458, Research Triangle Park, NC 27709, USA. [2]Department of Cell Biology, Duke University Medical Center, Durham NC 27710, USA.

*Author for correspondence (e-mail: mishina@niehs.nih.gov)

Accepted 26 July 2006

Whole-mount in situ analysis

Whole-mount in situ was performed as described (Belo et al., 1997). Probes used were brachyury (Wilkinson et al., 1990), *Lefty2* (Meno et al., 1999), *Foxf1* (Mahlapuu et al., 2001), *Bmp4* (Winnier et al., 1995), *Lim1* (Tsang et al., 2000), *Mox1* (Candia et al., 1992), *Uncx4.1* (Leitges et al., 2000), *Pax1* (Wallin et al., 1996), *Foxa2* (Sasaki and Hogan, 1994), *Tbx6* (Chapman et al., 1996), *Pcdh8* (Yamamoto et al., 2000), *Epha4* (Durbin et al., 1998) and noggin (McMahon et al., 1998).

Cell lineage analysis

Embryos were harvested in dissecting medium (Miura and Mishina, 2003). Cell lineage analysis was carried out as described previously (Wilson and Beddington, 1996). Briefly, a 0.5% stock solution of 1,1′-dioctadecyl-3,3,3′,3′-tetramethy-indocarbocyanine perchlorate (DiI) (Molecular Probes) in 100% ethanol was diluted tenfold with 0.3 M sucrose before use. DiI solution (0.05%) was sucked into a glass needle of 25 μm diameter (HUMAGEN). The tip of the needle softly touched the posterior region of the embryo, tore through the visceral endoderm and then DiI was released to label the mesoderm. These embryos were cultured with DR50 in a rotating glass bottle (BTC engineering) supplied with 5% O_2 and CO_2 balanced with N_2 at 37°C. After culture, embryos were placed in phosphate-buffered saline (PBS) and observed with a stereo-dissection microscope (Leica) under visible or ultra violet light, and imaged.

Inhibition of FGF signaling

SU5402 (CALBIOCHEM) was suspended in dimethyl sulfoxide (DMSO) (Sigma) as a 10 mM solution and kept at –20°C until use. E6.5-6.75 embryos were cultured with DR50 containing either SU5402 or DMSO for indicated lengths of time in rotating glass bottles.

Immunohistochemistry

Cultured embryos were washed in cold PBS and fixed with 4% paraformaldehyde overnight, dehydrated and embedded in paraffin. Sections (7 μm) were deparaffinized and stained with anti-phosphoErk1/2 antibody (Cell Signaling Technology) using an ABC kit (Vector Laboratories) according to manufacturers' protocols.

RESULTS

Bmpr-MORE embryos show multiple defects in mesodermal development

Bmpr-MORE embryos initiated gastrulation and were morphologically indistinguishable from control embryos at E6.5-6.75 (Davis et al., 2004). However, morphological defects were apparent in *Bmpr-MORE* embryos starting at E7.5. At the allantoic bud stage, control embryos had a distinctly formed amnion and chorion (Fig. 1A), while mutant embryos were characterized by a poorly formed amniotic fold and acute posterior curvature (Fig. 1A′). Amnion and chorion were not formed yet at the head-fold stage in *Bmpr-MORE* embryos (Fig. 1B′). In addition, a typical cardiac crescent did not develop in *Bmpr-MORE* embryos (Fig. 1C,C′ arrowheads). At E8.5, multiple defects were observed, including a striking lateral expansion of somites (Fig. 1D′,F′).

Histological sectioning at E8.5 revealed important aspects of these and other mesodermal phenotypes. In control embryos, somites developed as a single column on each side of the neural tube (Fig. 1F,G). In *Bmpr-MORE* embryos, ectopic mutant somites developed and extended laterally to form multiple irregular columns (Fig. 1F′,G′). The mutant somites formed typical ball-like epithelial-mesenchymal structures (Fig. 1F′,G′). In control embryos, LPM formed lateral to somites and medial to visceral yolk sac (Fig. 1E,G). In *Bmpr-MORE* embryos, lateral plate was apparently lacking, but cell masses were observed anterior and lateral to the paraxial somites and medial to the yolk sac, suggesting abnormal development of LPM (Fig. 1F′,G′). The heart formed at the most anterior end of normal embryos, but no analogous structure formed in *Bmpr-MORE* embryos (Fig. 1G,G′). Notochord was formed and expressed markers such as sonic hedgehog (Fig. 1G′) (Davis et al., 2004). The amnion was formed at this stage, but the allantois was notably small in the mutant embryos (Fig. 1H′).

Bmpr-MORE embryos were mosaic for recombined $Bmpr1a^{-/-}$ (mutant) cells and heterozygous cells (Davis et al., 2004). It is therefore important to know if both cell types distribute evenly or unevenly during development among all three germ layers. If there were a bias in their distribution, it might affect the mutant phenotype. We used a mouse line *R26R* to visualize mutant and heterozygous cells (Soriano, 1999). This is a reporter line for *Cre* recombinase, which marks those cells that have undergone recombination by expression of *lacZ*. As observed previously, both cell types were distributed evenly among tissues in control and mutant embryos (Fig. 1I-L) (Davis et al., 2004). These results indicate that *Bmpr1a* signaling in the epiblast did not restrict cells to or from any germ layer or major tissue in the early embryo. Thus, both mutant and heterozygous cells simultaneously traversed the primitive streak and ingressed into mesodermal tissues, resulting in a loss of BMPR1A signaling in most, but not all, epiblast-derived cells.

By contrast, *Sox2-Cre* mice catalyze complete recombination of *loxP* sequence in the epiblast (Fig. 1M,O) (Hayashi et al., 2002), allowing us to obtain embryos with total loss of BMPR1A signaling in the epiblast-derived tissues (Fig. 1N,P). Many of such mutant embryos showed a remarkably similar phenotype to *Bmpr-MORE* embryos, namely lateral expansion of somites (Fig. 1N,P). Having the similar phenotype both in *Bmpr-MORE* and *Sox2Cre*; $Bmpr1a^{flox/null}$ embryos implies that downstream targets of BMPR1A signaling act in a non-cell-autonomous manner to regulate early mouse epiblast development.

Correct patterning of ectopic somites and improper patterning of lateral plate mesoderm

To further explore how mutant somites were patterned, the expression for several markers for PXM development was examined. Normally, *Uncx4.1* (a marker for the caudal region of each somite) (Leitges et al., 2000) or *Dll1* (Bettenhausen et al., 1995) (a marker for caudal somite and presomitic mesoderm) was expressed as a column on each side of the embryo (Fig. 2A; data not shown). In mutant embryos, *Uncx4.1* or *Dll1* was expressed in multiple irregular columns on each side of the embryo, forming short mediolateral rows of expression domains (Fig. 2A′; data not shown). *Uncx4.1* was correctly expressed in caudal region of each somite in both control and mutant embryos (Fig. 2B,B′). The expression domain of *Epha4* (Durbin et al., 2000) or *Mesp2* (Saga et al., 1997) (markers of rostral presomitic mesoderm) was laterally broadened, indicating the expansion of presomitic mesoderm (Fig. 2C′; data not shown). *Mox1* (a paraxial mesoderm marker) (Candia et al., 1992), which is normally expressed in the somites (Fig. 2D,E), was not only expressed in expanded somites but also in cells of the LPM domain (Fig. 2D′,E′), suggesting the LPM had acquired PXM fate. The expression domain of *Pax1* (a marker for sclerotome) (Wallin et al., 1996) was also expanded in mutant embryos (Fig. 2F′). These data show that somites extended abnormally to the lateral edges of the embryo but individual somite were largely patterned correctly in *Bmpr-MORE* embryos.

By contrast, mutant LPM was very poorly patterned. *Foxf1* was normally expressed in LPM starting at E8.5 (Fig. 2G) (Mahlapuu et al., 2001). In *Bmpr-MORE* embryos, expression of *Foxf1* was patchy and often weak (Fig. 2G′). Some mutants did not express *Foxf1* at all, suggesting some variability of phenotype; this is possibly a result of the mosaic nature of the mutant embryos. *Bmp4* was expressed in allantois, the posterior primitive streak and LPM at E8.5 (Fig. 2H)

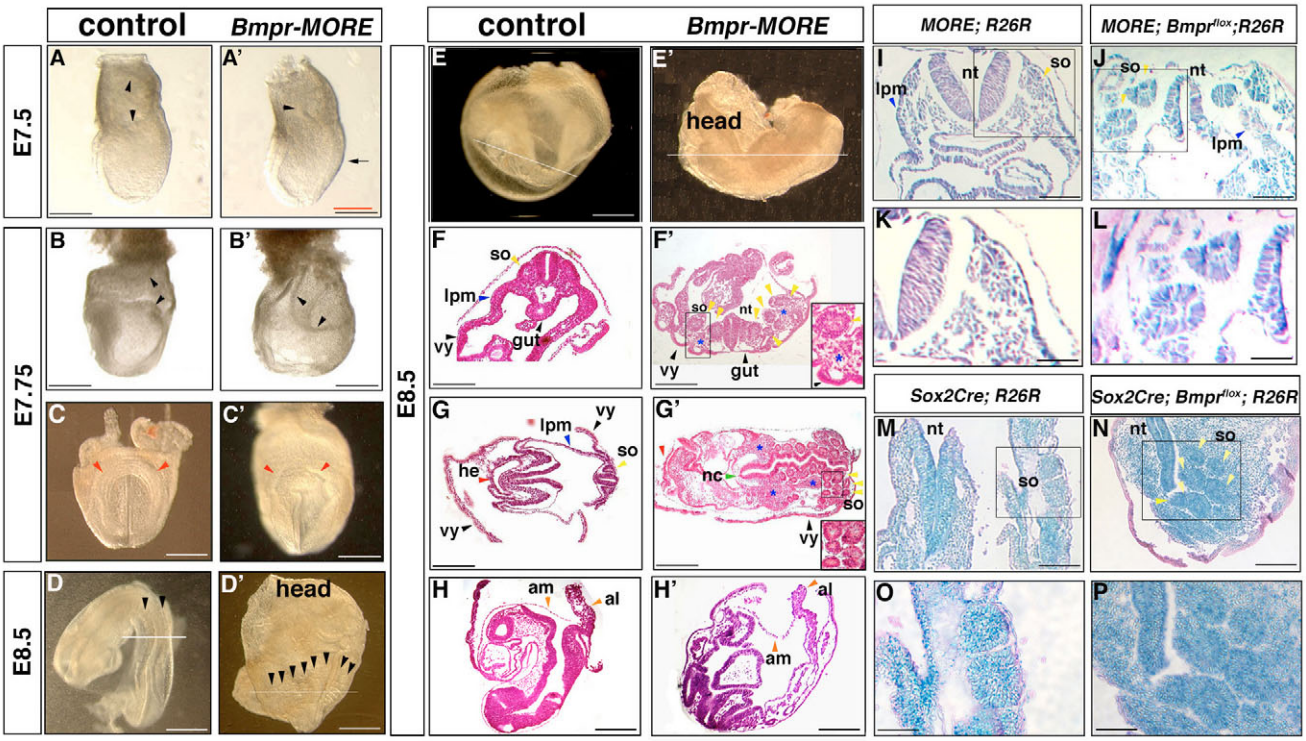

Fig. 1. Multiple defects of mesoderm development in *Bmpr-MORE* embryos. (**A-E'**) Whole-mount views. (A,A′) The no allantoic bud stage. Lateral view. Amnion and chorion were formed in control embryos at this stage (A, arrowheads). These tissues were not formed in *Bmpr-MORE* embryos (A′, arrowhead). An acute curvature was observed (A′, arrow). (B-C′) The head-fold stage. (B,B′) Lateral views. (C,C′) Frontal views. Amnion and chorion were not formed in *Bmpr-MORE* embryos (B′, arrowheads). Control embryos developed a typical heart crescent (C, arrowheads), whereas *Bmpr-MORE* embryos did not (C′, arrowheads). (D-E′) E8.5. (D) Dorsal view. Control embryos developed one column of somites on each side of the neural tube (arrowheads). (D′) Ventral view. Mutant embryos developed multiple columns of somites on each side (D′, arrowheads). White lines show approximate level of section for F,F′. (E,E′) Lateral view. White lines show approximate level of section for G or G′. (**F-H'**) Histological analyses (Hematoxylin and Eosin staining). (F,F′) Frontal section. In control embryos, lateral plate mesoderm (LPM) developed between somites (so) (yellow arrowhead) and visceral yolk sac (vy) (black arrowhead). In mutant embryos, mesenchymal cells (blue asterisks) accumulated between somites (yellow arrowheads) and visceral yolk sac (black arrowhead) in mutants (E′, see inset). Multiple somites developed to the lateral edge of the embryo (F′, yellow arrowheads). (G,G′) Transverse section. Between the somites (yellow arrowhead) and the visceral yolk sac (black arrowhead), LPM was observed in control embryos (blue arrowhead) (G). In *Bmpr-MORE* embryos, mesenchymal cell masses existed between the somites and the visceral yolk sac (G′, blue asterisks). Somites developed as multiple rows (G′, yellow arrowheads and inset). Heart (he) developed in the anterior region of control embryos (G, red arrowhead) but not in *Bmpr-MORE* embryos (G′, red arrowhead). The anterior half of the mutant embryo consists of neural tissues. Somites develop only in the posterior half of the mutant embryo. (H,H′) Sagittal section. Amnion (am) and allantois (al) were formed at this stage in mutant embryos (H′, orange arrowheads). (**I-L**) Transverse section of control or *Bmpr-MORE* embryos carrying *R26R* loci after staining for β-galactosidase activity. K and L are magnified images of I and J, respectively. Recombined (mutant) cells (blue) and heterozygous cells (pink) were distributed evenly among tissues such as somites (yellow arrowheads), LPM (blue arrowhead) or neural tube (nt). (**M-P**) Transverse section of control and *Sox2Cre*; *Bmpr1a*$^{flox/null}$ embryos carrying *R26R* loci after staining for β-galactosidase activity. Complete recombination of *R26R* was observed in the germ layers, namely in somites (O,P). *Sox2Cre*; *Bmpr1a*$^{flox/null}$ embryos developed multiple columns of somites (N,P, arrowheads). Scale bars: 170 μm for A; 200 μm for A′; 250 μm for B-C′,I,I′,M,N; 500 μm for D-E′,F-H′,K,L,O,P.

(Winnier et al., 1995). In *Bmpr-MORE* embryos, *Bmp4* was expressed in allantois and the primitive streak but not in LPM (Fig. 2H′). *Lim1* expression was normally observed in LPM at E7.75 (Fig. 2I) (Tsang et al., 2000). In *Bmpr-MORE* embryos, *Lim1* expression was either not expressed or lower than normal (Fig. 2I′; data not shown). These data indicate that *Bmpr1a* is required for proper patterning of LPM in normal development.

Delay in recruitment of prospective PXM

In *Bmpr-MORE* embryos, gastrulation initiated normally as described above. However, the primitive streak of mutant embryos was consistently shorter than that of control embryos during late stages of gastrulation. At the no allantoic bud stage (just prior to formation of the allantoic bud), brachyury was expressed in the entire primitive streak, the node and notochord in control embryos (Fig. 3A) (Wilkinson et al., 1990). In the notochord, the expression reached the anterior end of embryos (Fig. 3A). However, in *Bmpr-MORE* embryos, the most anterior domain of brachyury expression was in the distal region of the embryo (Fig. 3A′). In a control embryo at the allantoic bud stage, *Foxa2* was expressed in the node, notochord and anterior definitive endoderm (Fig. 3B) (Sasaki and Hogan, 1994). The node is formed at the most distal region of the primitive streak. In *Bmpr-MORE* embryos, the node was formed more proximally than in control embryos (Fig. 3B′). Similar observations were made using probes for noggin (Fig. 3C′) and *Lim1* (see Fig. S1A′ in the supplementary material) (McMahon et al., 1998; Tsang et al., 2000). These results indicate that the distoanterior extension of the primitive streak was defective in

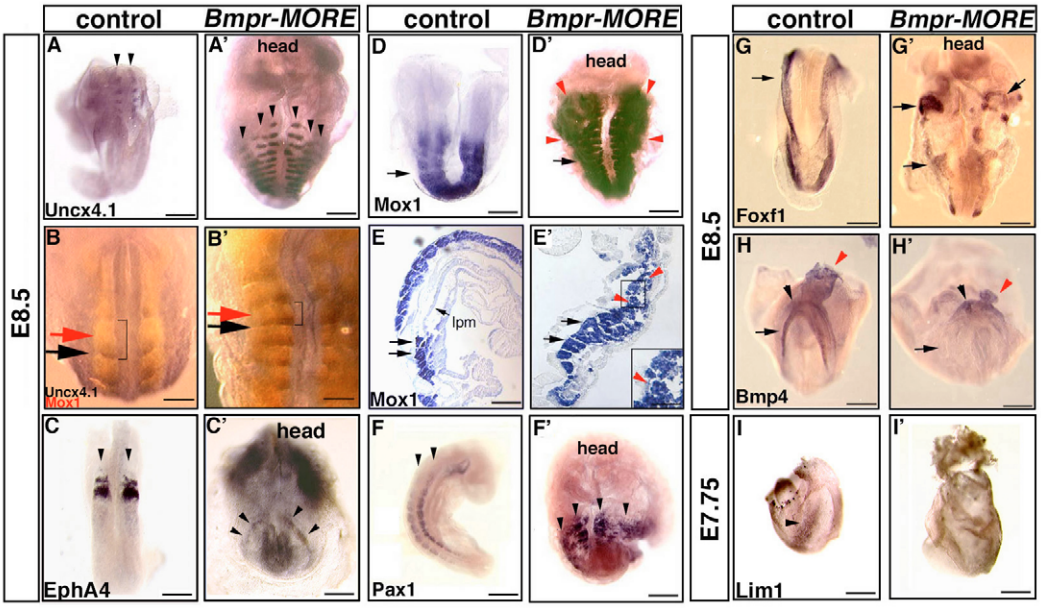

Fig. 2. Correct patterning of ectopic somites and improper patterning of LPM in *Bmpr-MORE* embryos. (**A-F′**) E8.5. Upper side is anterior. Dorsal or ventral view is shown for control or *Bmpr-MORE* embryos, respectively. *Uncx4.1*, a caudal marker of each somite, was expressed in a column on each side of control embryos (A, arrowheads). Three or more irregular columns of somites occurred and expressed *Uncx4.1* on each side of mutant embryos (A′, arrowheads). Double in situ analyses for *Uncx4.1* (black) and *Mox1* (yellow) (B,B′). *Mox1*, a marker of somites, was expressed in the entire region of each somite (red arrow) and *Uncx4.1* was expressed in the caudal part of each somite in both control and mutant embryos (black arrow). The bracket shows one somite. *Epha4* is a rostral presomitic mesoderm marker (C, arrowheads). The expression domain was expanded in *Bmpr-MORE* embryos (C′, arrowheads). *Mox1* was expressed in somites (D,E, arrows) but not in LPM in control embryos. In mutants, expression of *Mox1* was observed in somites (D′,E′, arrows) and in LPM (D′,E′, red arrowheads, see inset). (E,E′) Sections of D,D′. *Pax1* is expressed in sclerotome in control embryos (F, arrowheads). *Pax1* is expressed in expanded somites of *Bmpr-MORE* embryos (F′, arrowheads). (**G-I′**) Expression of LPM markers. (G,G′) Ventral view at E8.5. Upper side is anterior. *Foxf1* was expressed in LPM of control embryos (G, arrow). The expression of *Foxf1* was patchy and weak in *Bmpr-MORE* embryos (G′, arrows). (H-I′) Posterior view. In control embryos, *Bmp4* was expressed in LPM (arrow), proximal primitive streak (black arrowhead) and allantois (red arrowhead) (H). *Bmp4* was not expressed in mutant LPM (H′, arrow). Black and red arrowheads show the posterior primitive streak and allantois, respectively (H′). The expression of *Lim1* (I,I′, arrowhead) in migrating LPM. The *Lim1* was not expressed (I′) or was decreased in mutant embryos. Scale bars: 300 μm for A-A′,C,C′,D,D′,F,F′; 600 μm for B,B′; 250 μm for G-H′; 125 μm for I,I′,E,E′.

Bmpr-MORE embryos. However, by the head-fold stage, the primitive streak of *Bmpr-MORE* appeared to be fully elongated (Fig. 3D′; see Fig. S1B′ in the supplementary material). Thus, primitive streak extension was temporally delayed in *Bmpr-MORE* embryos during gastrulation**.**

Because the delay of primitive streak extension became apparent around the late streak stage, we examined if the production of LPM and/or PXM, which is normally induced by the late streak stage, was altered in *Bmpr-MORE* embryos. In control embryos, *Lefty2* was expressed in LPM and PXM at this stage (Fig. 3E) (Iratni et al., 2002; Meno et al., 1999). In *Bmpr-MORE* embryos, the expression domain for *Lefty2* was decreased and observed only in the proximal embryonic region (Fig. 3E′). *Tbx6* was also expressed in LPM and PXM at the late streak stage (see Fig. S1C in the supplementary material) (Chapman et al., 1996), but its expression was also decreased and observed in only the proximal embryonic region in *Bmpr-MORE* embryos (see Fig. S1C′ in the supplementary material). Thus, a reduced amount of LPM and/or PXM was induced in *Bmpr-MORE* embryos by the late-streak stage. These results suggest that the recruitment of prospective LPM and/or PXM to the primitive streak was delayed. This, in turn, caused a delay in the extension of the primitive streak in *Bmpr-MORE* embryos.

To further probe the temporal nature of mesoderm formation, we performed a cell lineage experiment using DiI, a tracer of living cells; this allowed us to label mesodermal cells with DiI, then to analyze their fate after culturing them for a defined period. DiI was injected into the proximal region of the primitive streak to label mesoderm cells of control or *Bmpr-MORE* embryos at the late streak stage (Fig. 4A,B). The embryos were then cultured for approximately 30 hours until the organogenesis stage (Fig. 4A′,B′). As expected, in control embryos, labeled cells contributed to lateral plate (3/3) and yolk sac (3/3) (Fig. 4A′,A″). Similarly, in all mutant embryos (5/5), labeled cells were distributed in regions of the embryo anterior and lateral to the paraxial region, but not to the somites (Fig. 4B′,B″). Labeled cells were also distributed in the yolk sac (3/5) (Fig. 4B′,B″). DiI was also injected into the anterior and distal region of the primitive streak of control or *Bmpr-MORE* embryos at the late streak stage (Fig. 4C,D). In control embryos, labeled cells contributed to somites and an axial tissue, which was probably axial mesoderm (3/3) (Fig. 4C′,C″). However, in the mutant embryos, labeled cells did not contribute to the paraxial region but rather to the anterior region and an axial tissue of the embryo (4/4) (Fig. 4D′,D″). These results indicate that the recruitment of prospective PXM had not occurred yet at the late streak stage in *Bmpr-MORE* embryos.

At the allantoic bud stage, *Lefty2* was normally expressed in migrating LPM and PXM cells (Fig. 3F). The two domains of expression were basically contiguous, suggesting that recruitment of prospective LPM and PXM occurs continuously. In *Bmpr-MORE* embryos, we found two domains of expression for *Lefty2* that were

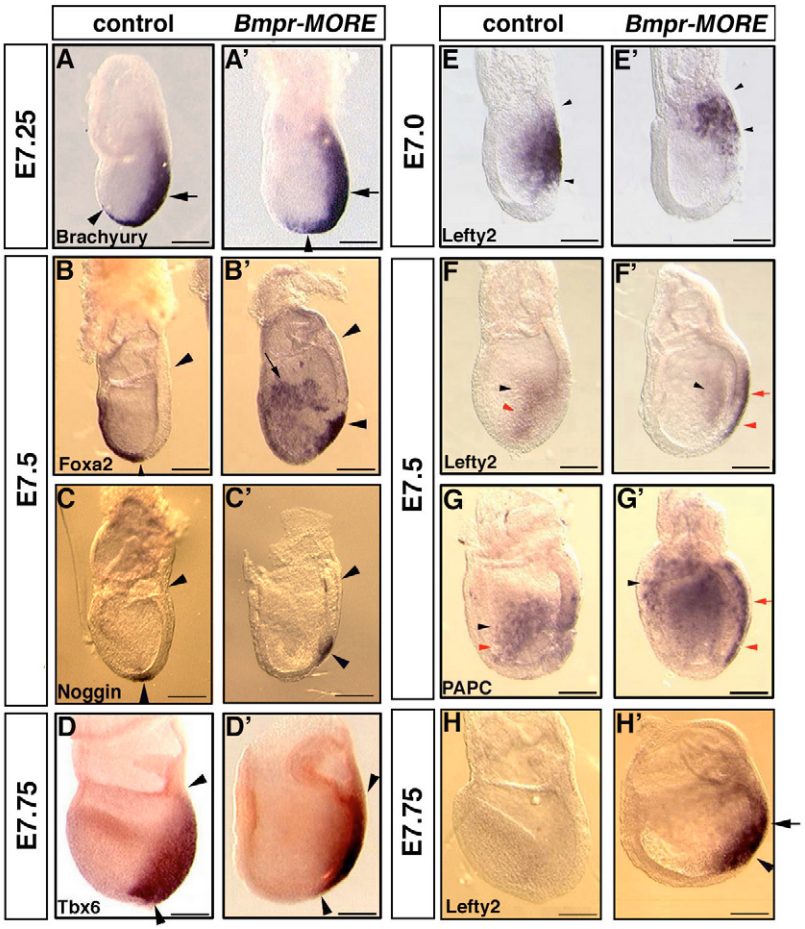

Fig. 3. Recruitment of prospective PXM is delayed during gastrulation in *Bmpr-MORE* embryos. (**A**,**A′**) No allantoic bud stage. Brachyury was expressed in the primitive streak (A, arrow), node and notochord of control embryos. The rostral end of the notochord was at the anterior of the embryo (A, arrowhead). The expression of *Brachyury* did not extend to the anterior in *Bmpr-MORE* embryos (A′, arrow and arrowhead). (**B-C′**) The early to late allantoic bud stage. *Foxa2* was expressed in the node (B, lower arrowhead) and notochord of control embryos. Upper arrowheads indicate embryonic/extra-embryonic border. As the node is formed at the distal region of the primitive streak, the length of the primitive streak corresponds to the length between two arrowheads. The length of the primitive streak of *Bmpr-MORE* embryos was shorter compared with that of control embryos (B′, arrowheads). Definitive endoderm develops in the mutant embryo (B′, arrow). (C,C′) Noggin was expressed in the node (lower arrowheads). The length of the primitive streak was shorter in mutant embryos (distance between arrowheads). (**D**,**D′**) The head-fold stage. (D) *Tbx6* was expressed in the mesoderm except axial mesoderm (between arrowheads). (D′) The length of the primitive streak appeared to be similar between control and *Bmpr-MORE* embryos (distance between arrowheads). (**E**,**E′**) The late streak stage. *Lefty2* was expressed in LPM and PXM (between arrowheads). (E) In *Bmpr-MORE*, *Lefty2* expression was decreased (E′, between arrowheads). (**F-G′**) The early to late allantoic bud stage. *Lefty2* was expressed in migrating LPM and PXM (F, black and red arrowheads, respectively). In *Bmpr-MORE*, the migrating LPM expressed *Lefty2* (F′, black arrowhead). More recently recruited mesoderm expressing *Lefty2* was observed at the middle and distal regions of the primitive streak (F′, red arrow and arrowhead, respectively). *Pcdh8* (PAPC on figure) was also expressed in LPM and PXM (G, black and red arrowheads, respectively). In *Bmpr-MORE*, the migrating LPM expressed *Pcdh8* (G′, black arrowhead). More recently recruited mesoderm expressing *Pcdh8* was observed at middle and distal regions of the primitive streak (G′, red arrow and arrowhead, respectively). *Lefty2* was not expressed at the head-fold stage in control embryos (**H**). In *Bmpr-MORE* embryos, *Lefty2* was still strongly expressed at distal and middle embryonic region (**H′**, arrowhead and arrow, respectively). Scale bars: 100 μm for A,A′,E,E′; 250 μm for B-D′; 200 μm for F-H′.

separated (Fig. 3F′). The more anterior domain most probably represented migrating LPM (Fig. 3F′). The other domain revealed mesoderm more recently recruited at the anterior and middle region of the primitive streak (Fig. 3F′). The same observations were made for the expression of paraxial procadherin (PCDH8), a trunk mesoderm marker at this stage (Fig. 3G′) (Yamamoto et al., 2000). *Lefty2* was actively transcribed even at the head-fold stage in *Bmpr-MORE* embryos (Fig. 3H′). These results further suggest that production of presumptive PXM was delayed in *Bmpr-MORE* embryos relative to control littermates of the same stage.

To determine if the mesoderm that was formed relatively late in the middle region of the primitive streak develops into PXM, we used DiI to trace the mesoderm of control and mutant embryos at the head-fold stage. As expected, cells in the anterior primitive streak contributed to somites in both control (2/2) and mutant embryos (3/3) (data not shown). Mesoderm cells in the middle region of the primitive streak contributed to LPM in control embryos (3/3) (Fig. 4E-E″). In *Bmpr*-MORE embryos, the mesoderm cells in the middle region of the primitive streak mainly contributed to somites (5/5) (Fig. 4F-F″) and only occasionally to LPM (1/5) and head mesenchyme (1/5). Importantly, these mesoderm cells largely contributed to the more lateral columns of somites (Fig. 4F′,F″). These results indicate that mesodermal cells formed relatively late in the middle region of the primitive streak were mostly committed to PXM. Collectively, our results suggest that the delay in the recruitment of prospective PXM results in a more proximal distribution of mesoderm cells with PXM character within the primitive streak, which probably leads to the lateral extension of somites in *Bmpr*-MORE embryos.

Inhibition of FGF signaling restores proper recruitment of prospective PXM and partially rescues the abnormal expansion of somites in *Bmpr-MORE* embryos

Embryos deficient for fibroblast growth factor receptor type 1 (FGFR1) do not form somites, indicating that FGF signaling is involved in the development of the PXM lineage (Ciruna and Rossant, 2001; Yamaguchi et al., 1994). In *Bmpr*-MORE embryos, LPM acquired PXM character (Fig. 2D′,E′). These observation led us to hypothesize that BMP signaling protects LPM from FGF signaling, which otherwise might cause the LPM to acquire PXM character. This hypothesis was tested by culturing E6.5-6.75 embryos in the presence of the FGFR1 antagonist SU5402 (Mohammadi et al., 1997). We reasoned that if the essential function

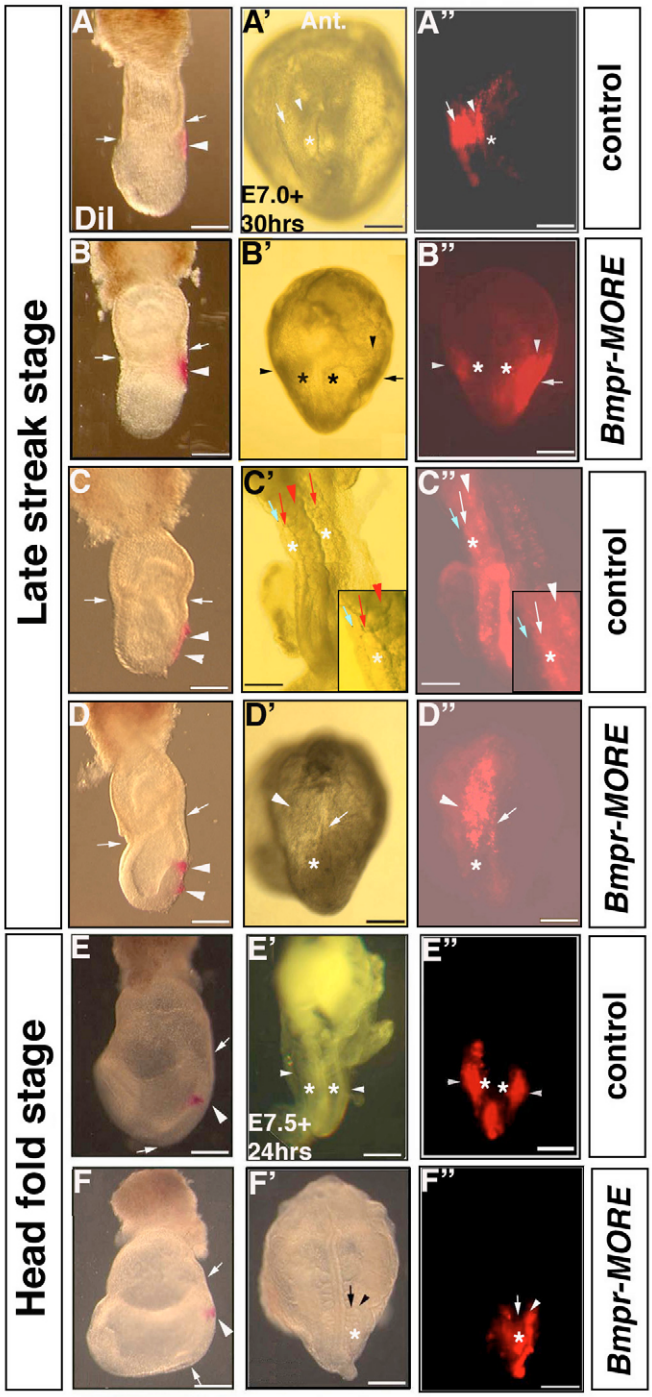

Fig. 4. Cell lineage analyses of control and mutant mesoderm cells. DiI was applied to the primitive streak mesoderm (**A**-**F**). After culture, embryos were observed under visible light (**A′**-**F′**) or ultra violet light (**A″-F″**). (A-B″) DiI was injected into the proximal region of the primitive streak (arrowheads) of control (A) or mutant embryos (B) at the late streak stage. Arrows indicate the embryonic/extra-embryonic border. Embryos injected with DiI were cultured for around 30 hours (A′,A′,B,B′, ventral view). Mesoderm cells derived from proximal primitive streak of control embryos contributed to lateral plate (A′, arrowhead and yolk sac, A″, arrow), but not to somites (A′,A″, asterisk). In *Bmpr-MORE* embryos, mesoderm cells derived from proximal primitive streak contributed to regions anterior and lateral to paraxial region (B′,B″, arrowheads and arrow, respectively) but apparently not to the paraxial region (B′,B″, asterisks). (C-D″) DiI was injected into the anterior-to-distal region of the primitive streak (arrowheads) of control (C) or mutant (D) embryos at the late streak stage. Embryos injected with DiI were cultured for around 30 hours (C′ and C″, dorsal view; D′ and D″, ventral view). (C′,C″) Mesoderm cells derived from the anterior-to-distal primitive streak of control embryos contributed to somites (asterisks) and to an axial structure (red arrows and arrowheads, respectively), but not to lateral plate (blue arrows) (see inset). (D′,D″) In *Bmpr-MORE* embryos, mesoderm cells derived from the anterior-to-distal primitive streak contributed to a region anterior to somites (arrowhead) and an axial structure (arrow). (E-F″) DiI was injected into the middle region of the primitive streak (E,F, arrowhead) of control and mutant embryos of the head-fold stage. Arrows indicate the length of the primitive streak. Embryos injected with DiI were cultured for around 24 hours. (E′,E″) Dorsal views. (F′,F″) Ventral view. (E′,E″) In control embryos, mesoderm cells derived from middle primitive streak contributed to lateral plate mesoderm (arrowheads), but not to somites (asterisks). (F′,F″) In *Bmpr-MORE* embryos, mesoderm cells derived from middle primitive streak mainly contributed to lateral row of somites (arrowhead) and fewer mesoderm cells contributed to medial row of somites (arrow). Scale bars: 100 μm for A-D; 250 μm for and E,F; 300 μm for A-B″,D-F″; 600 μm for C′,C″.

of *Bmpr1a* in terms of LPM development is to antagonize FGF signaling, SU5402 should be able to mitigate the abnormal patterning of LPM in *Bmpr-MORE* mutants.

Mutant and control embryos at E6.5-6.75 were cultured in DMEM with 50% rat serum (DR50) supplied with either dimethyl sulfoxide (DMSO) (vehicle for SU5402) or various concentration of SU5402. When cultured with DMSO or 10 μM SU5402 for around 20-24 hours, most control embryos reached a stage corresponding to the allantoic bud to head-fold stage (Fig. 5A; data not shown). Mutant embryos cultured with DMSO or 10 μM SU5402 showed poorly developed amniotic folds and a shorter primitive streak (Fig. 5A; data not shown). When cultured with 40 μM SU5402, all embryos showed abnormal development (see Fig. S2 in the supplementary material), as expected, with a strong reduction in FGFR1 activity. As a 50% inhibition of FGFR1 function is achieved at 10-20 μM (Mohammadi et al., 1997), we also tested the effect of 20 μM of SU5402. Control embryos developed normally at this concentration. By contrast, mutant embryos developed an amnion, chorion and allantois (12/12) (Fig. 5B,F). Moreover, the primitive streak appeared to extend normally in such embryos (Fig. 5B), suggesting that the recruitment of prospective PXM had occurred normally in *Bmpr-MORE* embryos in culture. Next, cultured embryos were tested for their expression of phosphorylated Erk1/2 to evaluate the level of signaling transduced by FGFR1 (Corson et al., 2003). The expression was observed most strongly in extra-embryonic ectoderm derived tissues and ectoplacental cone (Corson et al., 2003). In embryos cultured with DMSO, strong expression was observed in the chorion or amniotic fold and ectoplacental cone (Fig. 5C,D). When cultured with 20 μM SU5402, expression was still observed strongly in the ectoplacental cone. However, the expression in the chorion was significantly reduced, indicating that signaling from FGFR1 was inhibited in both control and *Bmpr-MORE* embryos (Fig. 5E,F). We then examined the expression of *Lefty2* in cultured embryos. As observed in vivo, the expression of *Lefty2* in mutant embryos cultured with DMSO was abnormal; the expression was shifted proximally and decreased (3/3) (Fig. 6B). However, when cultured with 20 μM SU5402, *Lefty2* was expressed

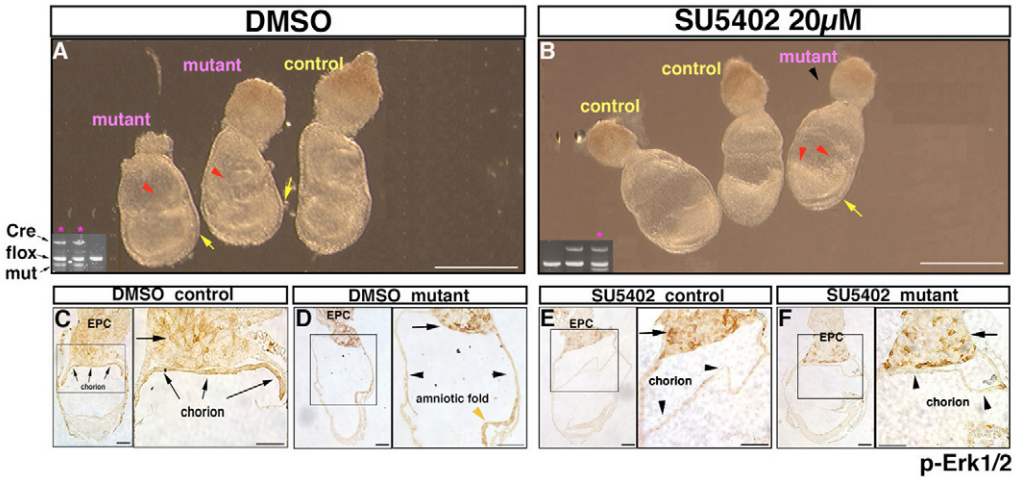

Fig. 5. Inhibition of FGF signaling by a specific antagonist for FGFR1 in *Bmpr-MORE* embryos. (**A**) Control embryos developed to the late streak to allantoic bud stage. *Bmpr-MORE* embryos showed a poorly developed amniotic fold (red arrowheads) and less extended primitive streak (yellow arrows) in culture, as was observed in vivo. Inset shows genotyping results for these embryos. Embryos positive for *Cre* and heterozygous for *Bmpr1a*-null allele are *Bmpr-MORE* embryos (inset, pink stars). (**B**) Control embryos developed to the allantoic bud stage. *Bmpr-MORE* embryos developed amnion, chorion and allantois (red arrowheads), and a well-extended primitive streak (yellow arrow). Embryos positive for *Cre* and heterozygous for *Bmpr1a-null* allele are *Bmpr-MORE* embryos (inset, pink star). (**C-F**) Cultured embryos stained with phospho-Erk1/2 antibody. (C) Control embryos cultured with DMSO. Ectoplacental cone (EPC) (arrow) and chorion (arrowheads) were strongly stained. (D) Mutant embryos cultured with DMSO. Ectoplacental cone (arrow) and the amniotic fold (orange arrowhead) showed strong expression. The extra-embryonic ectoderm in the ectoplacental cavity was weakly stained (black arrowheads). (E) Control embryos cultured with 20 μM SU5402. Expression in the ectoplacental cone was not affected (arrow), but that of the chorion was significantly decreased. (F) Mutant embryos cultured with 20 μM SU5402. Expression in the ectoplacental cone was not affected (arrow) but that of the chorion was significantly decreased (arrowheads). Scale bars: 500 μm for A,B; 100 μm for C-F.

at a normal level in mutant embryos (2/2) (Fig. 6D). These results indicate that inhibition of FGF signaling via reduction of FGFR1 activity rescued the delayed recruitment of prospective PXM in *Bmpr-MORE* embryos.

To further explore the impact of FGF signaling inhibition on somite development, we cultured embryos with 20 μM SU5402 for 48 hours. However, somite development was inhibited in such many embryos (see Fig. S2 in the supplementary material). Therefore, we cultured embryos with 20 μM SU5402 for 12-15 hours, removed the SU5402 by extensive washing, and continued to culture the embryos with DMSO for 48 hours in total. Under these conditions, somites developed normally (12/12) (Fig. 6G). Although somites were significantly expanded laterally in all mutant embryos cultured with DMSO (9/9) (Fig. 6F, see Fig. S3 in the supplementary material), treatment with SU5402 resulted in a variable level of rescue for somite development in six out of ten mutant embryos tested (Fig. 6H, see Fig. S3 in the supplementary material). Three mutant embryos developed only one or two rows of somites on both sides (Fig. 6H). In three other mutant embryos, the rescue in somite development was observed on one side of each embryo (see Fig. S3

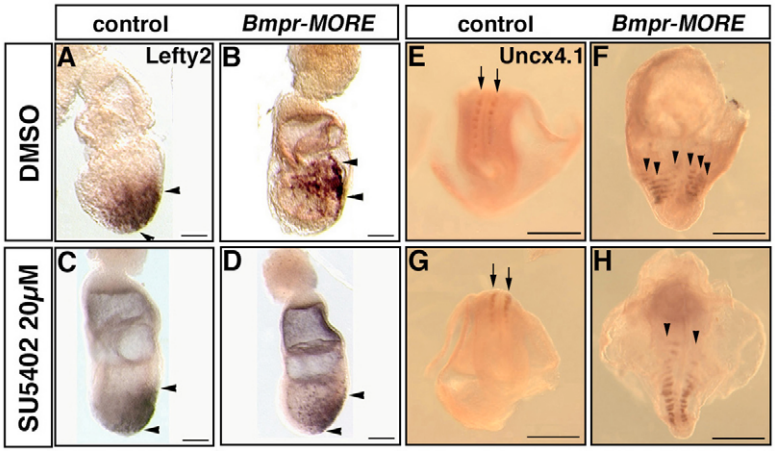

Fig. 6. Inhibition of FGF signaling partially rescues the development of somites in *Bmpr-MORE* embryos. (**A-D**) Control and *Bmpr-MORE* embryos at E6.5-6.75 grown in culture for 20-24 hours were examined for *Lefty2* expression. Control embryos cultured with DMSO normally expressed *Lefty2* (A, arrowheads). Mutant embryos cultured with DMSO showed a proximal shift and decreased expression of *Lefty2* (3/3) (B, arrowheads). Control embryos cultured with 20 μM SU5402 showed normal expression of *Lefty2* (C, arrowheads). Exposure to SU5402 normalized the expression of *Lefty2* in *Bmpr-MORE* embryos (2/2) (D, arrowheads). (**E-H**) Control and *Bmpr-MORE* embryos at E6.5-6.75 were cultured for around 48 hours and examined for the expression of *Uncx4.1*. (E) Control embryos cultured with DMSO normally expressed *Uncx4.1* (arrowheads). (F) Mutant embryos cultured with DMSO showed a significant expansion of somites to the lateral edge of the embryos (arrows) (*n*=9). (G) Control embryos were cultured with 20 μM SU5402 for 12-15 hours, extensively washed and then cultured with DMSO for around 48 hours in total. In this condition, somites developed normally (arrowheads). (H) Mutant embryos were cultured with 20 μM SU5402 for 12-15 hours, extensively washed and then with DMSO for around 48 hours in total. In six mutant embryos out of 10 tested, partial rescue of somite development was observed (arrowheads). Scale bars: 85 μm for A,B; 100 μm for C,D; 600 μm for E-H.

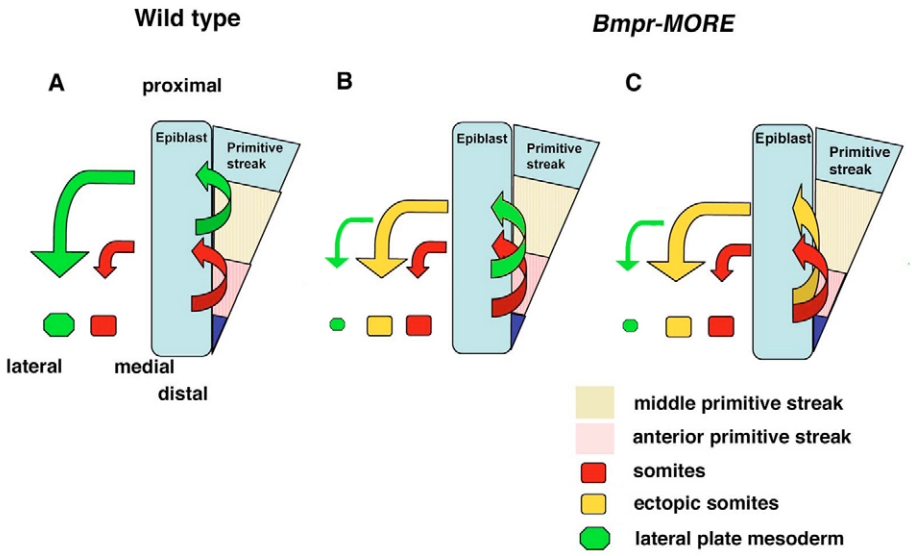

Fig. 7. Models for the role for BMPRIA in mesoderm development. (**A**) In wild-type embryos, epiblast cells that are recruited to the anterior primitive streak (red arrow) or to the middle primitive streak (green arrow) are fated to form somites (red square) or LPM (green hexagon), respectively, at the late streak stage. (**B**,**C**) Mutant embryos. (B) In mutant embryos, epiblast cells recruited to the anterior primitive streak probably form somites as in wild-type embryos (red arrows and red square). However, many epiblast cells passing through the middle primitive streak (green arrow), which should form LPM, change their fate to form ectopic somites (yellow arrow and yellow square); LPM is consequently reduced (green arrow and hexagon). (C) Alternatively, some of the prospective PXM cells are abnormally recruited to the middle primitive streak (yellow arrow) and form ectopic somites (yellow square). LPM is reduced owing to loss of contributing cells (green hexagon) resulting from reduced BMP signaling.

in the supplementary material). These data indicate that inhibition of FGF signaling during gastrulation partially rescued abnormal development of somites in *Bmpr-MORE* embryos.

It was possible that the observed rescue of somite development was due to normal development of the LPM in *Bmpr-MORE* embryos. Therefore, we also examined the expression of *Foxf1* in embryos cultured as described above. *Foxf1* was not expressed in these mutant embryos, indicating that inhibition of FGF signaling did not rescue the abnormal development of the LPM (data not shown).

DISCUSSION

In this paper, we have shown that BMPRIA in the epiblast is essential for proper recruitment of epiblast cells into the primitive streak. This, in turn, has important consequences for development of the mesodermal region of the embryo, such as the somites.

Bmpr-MORE embryos at the allantoic bud stage showed a characteristic morphology: an acute curvature in the posterior side, which was due to a delay of primitive streak extension. Our results indicate that recruitment of prospective PXM that normally occurs during the mid to late streak stage was delayed and took place during the allantoic bud to head fold stage in *Bmpr-MORE* embryos. Normally, the prospective PXM population arises mainly at the anterior primitive streak. Our results indicate mesoderm cells with PXM character arise in the middle in addition to the anterior part of the primitive streak. The distoproximal order of the prospective mesoderm cells within the primitive streak is maintained during ingression of cells from the primitive streak into the mesoderm (Smith et al., 1994). Presumably, PXM cells in the middle part of the primitive streak migrate more laterally and PXM cells at the distal part of the primitive streak migrate more medially, thus causing an altered morphogenesis of somites in *Bmpr-MORE* embryos.

We propose two possible models to explain the mechanism of how ectopic somites develop in *Bmpr-MORE* mutant embryos. The first model proposes that loss of BMP signaling causes a fate change of epiblast cells passing through the middle primitive streak, which would normally form the LPM, and that these cells consequently form ectopic somites (Fig. 7B, yellow arrow). The second model posits that the delay of recruitment in *Bmpr-MORE* embryos causes abnormal morphogenetic movement of prospective PXM cells upon recruitment to the primitive streak (Fig. 7C). Normally, these cells are recruited to the anterior primitive streak and exit from the anterior primitive streak (Fig. 7A, red arrow). In the mutant embryos, these cells are abnormally recruited to the middle primitive streak to form ectopic somites (Fig. 7C, yellow arrow).

FGF signaling induces PXM patterning via expression of brachyury and *Tbx6* (Ciruna and Rossant, 2001). However, inhibition of FGF signaling in *Bmpr-MORE* embryos restored normal timing of prospective PXM recruitment. Together, these data indicate that FGF signaling negatively regulates recruitment of prospective PXM cells but is required for their patterning. Interestingly, we found that BMPs do not regulate the recruitment of prospective LPM cells, but they are essential for LPM patterning (this study). These observations suggest that a mechanism(s) might be present that are responsible for controlled allocation of mesoderm and thus for successful establishment of mouse body plan.

Control embryos treated with 20 μM SU5402 developed apparently normally up to the allantoic bud stage. However, *Fgf8*-deficient mice exhibit a marked decrease in migration of mesoderm cells out of the primitive streak during gastrulation (Sun et al., 1999). Probably, the concentration of SU5402 used here does not sufficiently inhibit FGF signaling to elicit this migratory defect.

It is unlikely that BMP signaling directly inhibits FGF signaling. In *Bmpr-MORE* embryos, the phosphorylation of ERK1 and ERK2, major signal transducers of FGF signaling appears at the normal level. In addition, *Snai1*, one of target genes of FGF signaling, is expressed normally in mutant embryos (data not shown). Rather, downstream targets of BMP and FGF signaling are probably involved in antagonistic effects.

Through the analyses of *Bmpr-MORE* embryos, we identified novel functions of BMP signaling in gastrulation. However, many issues remain to be addressed. The mechanism that explains delayed recruitment of epiblast cells (prospective PXM) is unknown, although we showed that BMP and FGF signaling have antagonistic effects on this process. The identification of such mechanisms and the assessment of their functions are crucial for a more thorough understanding of mouse gastrulation.

We thank Phillipe Soriano and Michelle Tallquist for providing us *Mox2-cre* and R26R transgenic mice; and B. G. Herrmann, H. Hamada, P. Carlsson, B. Hogan, R. P. Harvey, C. V. Wright, A. Kispert, R. Balling, D. L. Chapman, Y. Saga and E. M. Robertis for in situ probes. We also thank Xin Sun, Michelle Tallquist, Manas Ray, Mitch Eddy, Akihiko Shimono, Yu-Ping Yang, Brigid Hogan and Liz Lacy for critical reading of this manuscript; and Noriko Osumi and Akihiko Shimono for information about the cell trace experiments. This research was supported by the Intramural Research Program of the NIH, National Institute of Environmental Health Sciences to Y.M. and by NIH awards to J.K. (R01DE013674 and P01HD39948).

Supplementary material

Supplementary material for this article is available at
http://dev.biologists.org/cgi/content/full/133/19/3767/DC1

References

Belo, J. A., Bouwmeester, T., Leyns, L., Kertesz, N., Gallo, M., Follettie, M. and De Robertis, E. M. (1997). Cerberus-like is a secreted factor with neutralizing activity expressed in the anterior primitive endoderm of the mouse gastrula. *Mech. Dev.* **68**, 45-57.

Bettenhausen, B., Hrabe de Angelis, M., Simon, D., Guenet, J. L. and Gossler, A. (1995). Transient and restricted expression during mouse embryogenesis of Dll1, a murine gene closely related to Drosophila Delta. *Development* **121**, 2407-2418.

Candia, A. F., Hu, J., Crosby, J., Lalley, P. A., Noden, D., Nadeau, J. H. and Wright, C. V. (1992). Mox-1 and Mox-2 define a novel homeobox gene subfamily and are differentially expressed during early mesodermal patterning in mouse embryos. *Development* **116**, 1123-1136.

Chapman, D. L., Agulnik, I., Hancock, S., Silver, L. M. and Papaioannou, V. E. (1996). Tbx6, a mouse T-Box gene implicated in paraxial mesoderm formation at gastrulation. *Dev. Biol.* **180**, 534-542.

Ciruna, B. and Rossant, J. (2001). FGF signaling regulates mesoderm cell fate specification and morphogenetic movement at the primitive streak. *Dev. Cell* **1**, 37-49.

Corson, L. B., Yamanaka, Y., Lai, K. M. and Rossant, J. (2003). Spatial and temporal patterns of ERK signaling during mouse embryogenesis. *Development* **130**, 4527-4537.

Davis, S., Miura, S., Hill, C., Mishina, Y. and Klingensmith, J. (2004). BMP receptor IA is required in the mammalian embryo for endodermal morphogenesis and ectodermal patterning. *Dev. Biol.* **270**, 47-63.

Durbin, L., Brennan, C., Shiomi, K., Cooke, J., Barrios, A., Shanmugalingam, S., Guthrie, B., Lindberg, R. and Holder, N. (1998). Eph signaling is required for segmentation and differentiation of the somites. *Genes Dev.* **12**, 3096-3109.

Durbin, L., Sordino, P., Barrios, A., Gering, M., Thisse, C., Thisse, B., Brennan, C., Green, A., Wilson, S. and Holder, N. (2000). Anteroposterior patterning is required within segments for somite boundary formation in developing zebrafish. *Development* **127**, 1703-1713.

Hayashi, S., Lewis, P., Pevny, L. and McMahon, A. P. (2002). Efficient gene modulation in mouse epiblast using a Sox2Cre transgenic mouse strain. *Mech. Dev.* **119**, S97-S101.

Hornbruch, A., Summerbell, D. and Wolpert, L. (1979). Somite formation in the early chick embryo following grafts of Hensen's node. *J. Embryol. Exp. Morphol.* **51**, 51-62.

Iratni, R., Yan, Y. T., Chen, C., Ding, J., Zhang, Y., Price, S. M., Reinberg, D. and Shen, M. M. (2002). Inhibition of excess nodal signaling during mouse gastrulation by the transcriptional corepressor DRAP1. *Science* **298**, 1996-1999.

Kinder, S. J., Tsang, T. E., Quinlan, G. A., Hadjantonakis, A. K., Nagy, A. and Tam, P. P. (1999). The orderly allocation of mesodermal cells to the extraembryonic structures and the anteroposterior axis during gastrulation of the mouse embryo. *Development* **126**, 4691-4701.

Kishigami, S. and Mishina, Y. (2005). BMP signaling and early embryonic patterning. *Cytokine Growth Factor Rev.* **16**, 265-278.

Lawson, K. A., Meneses, J. J. and Pedersen, R. A. (1991). Clonal analysis of epiblast fate during germ layer formation in the mouse embryo. *Development* **113**, 891-911.

Leitges, M., Neidhardt, L., Haenig, B., Herrmann, B. G. and Kispert, A. (2000). The paired homeobox gene Uncx4.1 specifies pedicles, transverse processes and proximal ribs of the vertebral column. *Development* **127**, 2259-2267.

Mahlapuu, M., Ormestad, M., Enerback, S. and Carlsson, P. (2001). The forkhead transcription factor Foxf1 is required for differentiation of extra-embryonic and lateral plate mesoderm. *Development* **128**, 155-166.

McMahon, J. A., Takada, S., Zimmerman, L. B., Fan, C. M., Harland, R. M. and McMahon, A. P. (1998). Noggin-mediated antagonism of BMP signaling is required for growth and patterning of the neural tube and somite. *Genes Dev.* **12**, 1438-1452.

Meno, C., Gritsman, K., Ohishi, S., Ohfuji, Y., Heckscher, E., Mochida, K., Shimono, A., Kondoh, H., Talbot, W. S., Robertson, E. J. et al. (1999). Mouse Lefty2 and zebrafish antivin are feedback inhibitors of nodal signaling during vertebrate gastrulation. *Mol. Cell* **4**, 287-298.

Mishina, Y. (2003). Function of bone morphogenetic protein signaling during mouse development. *Front. Biosci.* **8**, d855-d869.

Mishina, Y., Suzuki, A., Ueno, N. and Behringer, R. R. (1995). Bmpr encodes a type I bone morphogenetic protein receptor that is essential for gastrulation during mouse embryogenesis. *Genes Dev.* **9**, 3027-3037.

Mishina, Y., Hanks, M. C., Miura, S., Tallquist, M. D. and Behringer, R. R. (2002). Generation of Bmpr/Alk3 conditional knockout mice. *Genesis* **32**, 69-72.

Miura, S. and Mishina, Y. (2003). Whole-embryo culture of E5.5 mouse embryos: development to the gastrulation stage. *Genesis* **37**, 38-43.

Mohammadi, M., McMahon, G., Sun, L., Tang, C., Hirth, P., Yeh, B. K., Hubbard, S. R. and Schlessinger, J. (1997). Structures of the tyrosine kinase domain of fibroblast growth factor receptor in complex with inhibitors. *Science* **276**, 955-960.

Parameswaran, M. and Tam, P. P. (1995). Regionalisation of cell fate and morphogenetic movement of the mesoderm during mouse gastrulation. *Dev. Genet.* **17**, 16-28.

Saga, Y., Hata, N., Koseki, H. and Taketo, M. M. (1997). Mesp2: a novel mouse gene expressed in the presegmented mesoderm and essential for segmentation initiation. *Genes Dev.* **11**, 1827-1839.

Sasaki, H. and Hogan, B. L. (1994). HNF-3 beta as a regulator of floor plate development. *Cell* **76**, 103-115.

Smith, J. L., Gesteland, K. M. and Schoenwolf, G. C. (1994). Prospective fate map of the mouse primitive streak at 7.5 days of gestation. *Dev. Dyn.* **201**, 279-289.

Soriano, P. (1999). Generalized lacZ expression with the ROSA26 Cre reporter strain. *Nat. Genet.* **21**, 70-71.

Sun, X., Meyers, E. N., Lewandoski, M. and Martin, G. R. (1999). Targeted disruption of Fgf8 causes failure of cell migration in the gastrulating mouse embryo. *Genes Dev.* **13**, 1834-1846.

Tallquist, M. D. and Soriano, P. (2000). Epiblast-restricted Cre expression in MORE mice: a tool to distinguish embryonic vs. extra-embryonic gene function. *Genesis* **26**, 113-115.

Tam, P. P. and Quinlan, G. A. (1996). Mapping vertebrate embryos. *Curr. Biol.* **6**, 104-106.

Tam, P. P. and Behringer, R. R. (1997). Mouse gastrulation: the formation of a mammalian body plan. *Mech. Dev.* **68**, 3-25.

Tonegawa, A. and Takahashi, Y. (1998). Somitogenesis controlled by Noggin. *Dev. Biol.* **202**, 172-182.

Tsang, T. E., Shawlot, W., Kinder, S. J., Kobayashi, A., Kwan, K. M., Schughart, K., Kania, A., Jessell, T. M., Behringer, R. R. and Tam, P. P. (2000). Lim1 activity is required for intermediate mesoderm differentiation in the mouse embryo. *Dev. Biol.* **223**, 77-90.

Wallin, J., Eibel, H., Neubuser, A., Wilting, J., Koseki, H. and Balling, R. (1996). Pax1 is expressed during development of the thymus epithelium and is required for normal T-cell maturation. *Development* **122**, 23-30.

Wilkinson, D. G., Bhatt, S. and Herrmann, B. G. (1990). Expression pattern of the mouse T gene and its role in mesoderm formation. *Nature* **343**, 657-659.

Wilson, V. and Beddington, R. S. (1996). Cell fate and morphogenetic movement in the late mouse primitive streak. *Mech. Dev.* **55**, 79-89.

Winnier, G., Blessing, M., Labosky, P. A. and Hogan, B. L. (1995). Bone morphogenetic protein-4 is required for mesoderm formation and patterning in the mouse. *Genes Dev.* **9**, 2105-2116.

Yamaguchi, T. P., Harpal, K., Henkemeyer, M. and Rossant, J. (1994). fgfr-1 is required for embryonic growth and mesodermal patterning during mouse gastrulation. *Genes Dev.* **8**, 3032-3044.

Yamamoto, A., Kemp, C., Bachiller, D., Geissert, D. and De Robertis, E. M. (2000). Mouse paraxial protocadherin is expressed in trunk mesoderm and is not essential for mouse development. *Genesis* **27**, 49-57.